A polyene chain of canthaxanthin investigated by temperature-dependent resonance Raman spectra and density functional theory (DFT) calculations*

Chen Yuan-Zheng (陈元正)[a)b)], Li Shuo(李 硕)[a)], Zhou Mi(周 密)[a)b)], Li Zuo-Wei(里佐威)[a)], and Sun Cheng-Lin(孙成林)[a)†]

[a)] *College of Physics, Jilin University, Changchun* 130012, *China*

[b)] *State Key Laboratory of Superhard Materials, Jilin University, Changchun* 130012, *China*

(Received 13 November 2012; revised manuscript received 4 January 2013)

We report on a temperature-dependent resonance Raman spectral characterization of the polyene chain of canthaxanthin. It is observed that all vibrational intensities of the polyene chain are inversely proportional to temperature, which is analyzed by the resonance Raman effect and the coherent weakly damped electron/lattice vibrations. The increase in intensity of the CC overtone/combination relative to the fundamental with temperature decreasing is detected and discussed in terms of electron/phonon coupling and the activation energy $U_{\rm op}$. Moreover, the polyene chain studies using the density functional theory B3LYP/6-31G* level reveal a prominent peak at 1525 cm^{-1} consisting of two closely spaced modes that are both dominated by C=C stretching coordinates of the polyene chain.

Keywords: canthaxanthin, density functional theory, polyene chain, Raman spectra

PACS: 33.20.Fb **DOI:** 10.1088/1674-1056/22/8/083301

1. Introduction

Carotenoids play an important role in various physiological processes of critical importance for life in its present form.[1–3] In most natural processes, they are assumed to play the roles of energy and electron carriers. The increasing interest in the chemistry of carotenoids, such as β-carotene, xanthophylls, and canthaxanthin, relates to many functions of these biomolecules with their rich structural diversities.[4–6] Carotenoids, containing a π-electron conjugated double bond, are chemically linear chain polyenic compounds, which have multiple important functions in photo-protection, light-harvesting, and photo-conducting devices.[7–9]

Canthaxanthin, as a chemically simple π-conjugated polyene, with a polyene chain consisting of the sequences of carbon–carbon bonds ($\cdots$ –C=C–C=$\cdots$), is characterized by a strong electron–phonon coupling due to the delocalized π electrons.[10] The density of mobile π-electrons between the adjacent carbon sites in the polyene chain strongly modulates the strength of their covalent bonding, giving rise to a high electron/phonon coupling and an effective nonlinearity for the lattice motion. In fact, these properties directly relate to their polyene chain structures, which are sensitive to the molecular environments around their polyene chain. During the last several decades, it has attracted special attention and was considered as a unique research object.[11,12] Despite considerable efforts, the temperature effect on the polyene chain still contains some mysterious aspects, thereby attracting a lot of attention. The main reason for such a situation is that in real samples, disorder has always obscured the true process of the intrinsic excitations of the polymer chain.

As is well known, molecular spectroscopy, particularly resonance Raman spectroscopy, has been proved to be a very powerful technique with which a wide range of compounds containing extended polyene –(CH=CH)$_n$- sequences[13,14] have been successfully investigated. Meanwhile, density functional theory (DFT), as a quantum chemical calculated theory, has shown good performance in investigating the structural characteristics of organic molecules.[15] In the present paper, special attention is paid to the effect of temperature on the polyene chain of canthaxanthin by the temperature-dependent resonance Raman spectrum. In addition, the optimizations of geometry and frequency calculation of canthaxanthin are performed by using the DFT B3LYP in conjunction with the 6-31G* basis set to improve our understanding of the polyene chain

2. Experimental methods

Canthaxanthin was purchased from Sigma–Aldrich, stored at –20 °C in the dark, and used without further purification. 1, 2-dichloroethane served as reagents of analytical grade. Canthaxanthin (0.0027 g) was dissolved in 10-ml 1, 2-dichloroethane, and the concentration of canthaxanthin was 10^{-4} M. All Raman spectra were measured us-

*Project supported by the National Natural Science Foundation of China (Grant Nos. 10974067 and 11104107), the Program of Jilin Province Science and Technology Department, China (Grant Nos. 20090534 and 20101508), and the China Postdoctoral Science Foundation, China (Grant No. 20110491320).

†Corresponding author. E-mail: chenglin@mail.jlu.edu.cn

© 2013 Chinese Physical Society and IOP Publishing Ltd

ing a microscope-based Raman spectrometer Renishaw inVias with 514.5 nm for excitation (Spectra-Physics 160 M argon ion laser), backscattered and collected using its 5× object lenses. The spectra were collected at a lower laser power in order to avoid the local heating effect. The laser power was 6 MW, and the typical integration time was 30 s for one measurement. The temperature-dependent Raman spectra were recorded in a temperature range of 20 °C−−180 °C (to minus 180 °C). A temperature-controlled Raman spectrometer (Linkam thms600) was used to control the temperature of the samples.

3. Computational method

Quantum chemical calculations were performed with the program package GAUSSIAN03.[16] The DFT has been proved to be extremely useful in treating electronic structure calculations. The geometry and frequency of the monomer were optimized by using the DFT B3LYP in conjunction with the 6-31G* basis set. The force constants were scaled with a set of global scaling factors as described previously.[17,18] The optimized structural parameters were used in the subsequent vibrational frequency calculations by which all the stationary points are also the minima. Redundant internal coordinates were generated using the program MOLDEN, and the Raman activities were calculated analytically.

4. Results and discussion

4.1. Temperature-dependent resonance Raman spectral analysis

The Raman spectra of canthaxanthin dissolved in 1, 2-dichloroethane in a temperature range of 20 °C−−180°C are presented in Fig. 1 and exhibit two intensive fundamentals with frequencies of 1520 cm^{-1} and 1155 cm^{-1}, respectively. These two peaks could be assigned to the totally symmetric C=C stretching υ_1 and C–C stretching υ_2 modes. The other bands, located at about 2310 cm^{-1}, 2670 cm^{-1}, and 3050 cm^{-1}, are reasonably assigned as overtone $2\upsilon_2$, combination $\upsilon_1 + \upsilon_2$, and overtone $2\upsilon_1$, respectively.[19,20] It is reported that the UV-Vis absorption spectra of canthaxanthin are generally shaped by a strong band in a range from 350 nm to 600 nm.[21] This absorption band is attributed to the $A_g^{-1} \rightarrow B_g^{-1}$ transition. It means that the excitation wavelengths (514.5 nm) employed in our experiment lie in the envelope of the ground state and the allowed lowest electronic state of canthaxanthin. So, a resonance Raman spectrum of canthaxanthin is obtained in our experiment. The vibrational intensity of the linear polyene molecule is determined mainly by the resonance Raman effect and the coherent weakly damped electron–lattice vibration. So here we discuss the temperature relation between Raman intensities and these two factors. With temperature decreasing, the sample solution density increases and the intermolecular distance shortens. As a result, the space of molecular rotation and the space of molecular vibration are reduced and the molecular thermal disorder is also weakened accordingly, thereby effectively improving the molecular structural order and enhancing the coherent weakly damped electron–lattice vibrations. The improvement on the molecular structural order extends the degree of the π-electron delocalization, lengthens the molecular effective conjugation, and causes the electronic absorption band of polyenes to be red-shifted with frequency decreasing between 514.5-nm excitation band and electronic absorption band. As a result, the resonance Raman effect is enhanced, which induces the intensities of all bands to be enhanced (Fig. 1).

Furthermore, we observe the intensity of the CC overtone/combination relative to the fundamental increases with

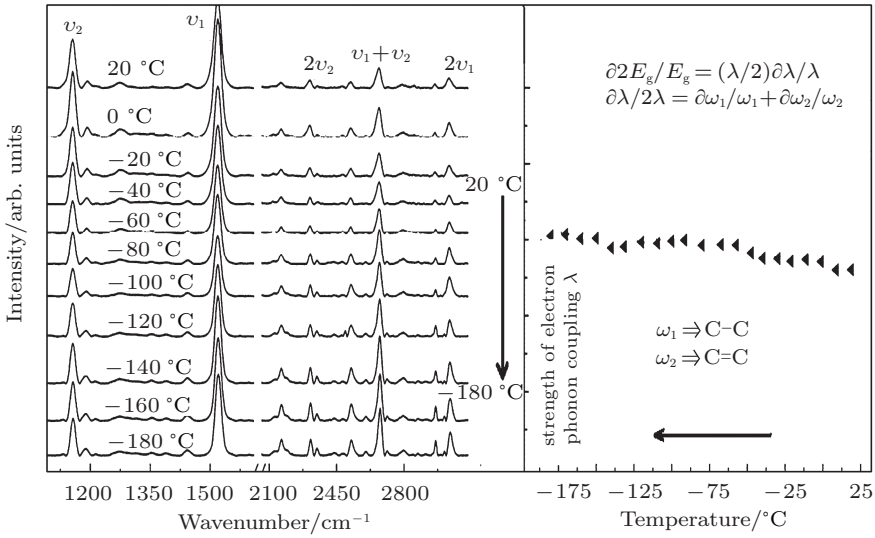


Fig. 1. Resonance Raman spectra of canthaxanthin dissolved in 1, 2-dichloroethane in a temperature range of 20 °C−−180 °C (left), and temperature dependence of the strength of the electron–phonon coupling (right).

temperature decreasing in Fig. 2. Firstly, we consider the electron/phonon coupling mechanism described by Castiglioni *et al.*[22] The parameter λ characterizes the strength of electron/phonon coupling and drives the phonon frequency. The relationship between the energy gap of the Peierls chain and the electron–phonon parameter λ is $E_g \approx \exp(-\lambda/2)$.[23] The Raman frequency υ is related to λ by the "product rule". For those small temperature-induced changes in the energy gap and the Raman frequencies, we have[24]

$$\partial E_g/E_g = (1/2\lambda)(\partial\lambda/\lambda), \tag{1}$$

$$\partial\lambda/\lambda = \partial\upsilon_1/\upsilon_1 + \partial\upsilon_2/\upsilon_2, \tag{2}$$

$$E_g = h\upsilon. \tag{3}$$

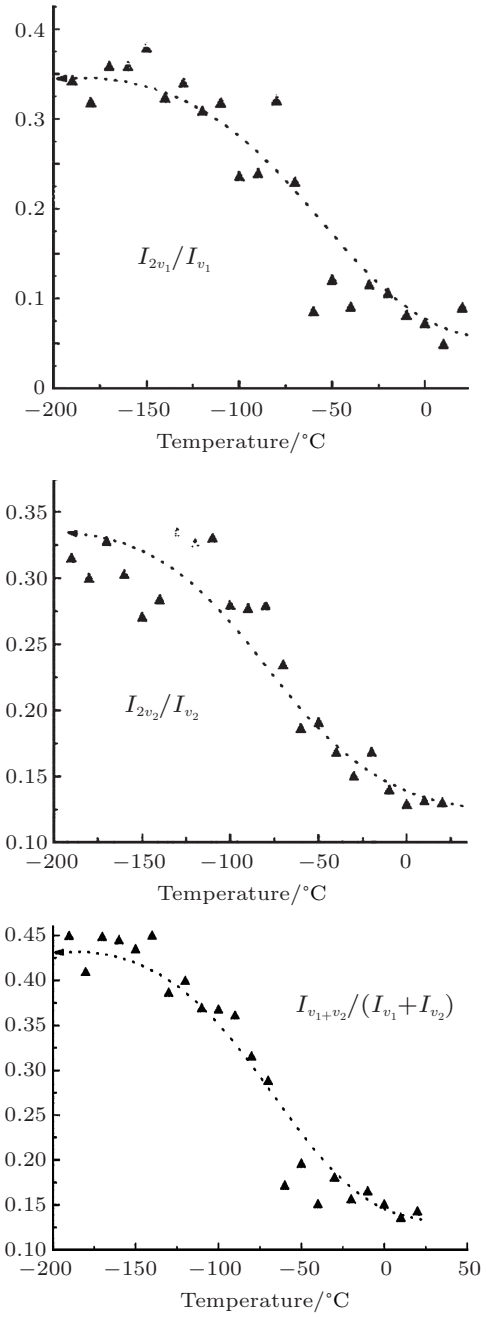


Fig. 2. Variations of relative intensity changes of the CC overtone/combination with temperature.

Here, $h = 6.626 \times 10^{-34}$; $\upsilon_1 = 1520$ cm^{-1} (C=C), and $\upsilon_2 = 1155$ cm^{-1} (C–C); $\partial\upsilon$ is frequency difference between the different temperatures. The electron–phonon parameter λ can be calculated from Eqs. (1)–(3) with these data. As shown in Fig. 1(b), the λ slightly increases with temperature decreasing meaning that the strength of electron/phonon coupling also slightly strengthens with the temperature decreasing. Parker *et al.*[25] reported that the substantial reduction in intensity of the overtone/combination peak of β–carotene relative to the fundamentals with excitation wavelength increasing resulted from electron/phonon coupling. Their observation provides the fundamental case with a different enhancement mechanism and reveals that the electron/phonon coupling process advanced is the clear candidate. In our observed case for canthaxanthin as a similar carotenoid, it is reasonable to conclude that the λ strengthening as a candidate factor interprets the fact that the CC overtone/combination relative to the fundamentals increases with temperature decreasing.

Secondly, the Boltzmann distribution of a set of molecules at vibrational levels υ_j gives the following relationships between the intensity and temperature for Stokes Raman lines:[26]

for a fundamental υ_j

$$I \approx [1 - \exp(-1.44\upsilon_j/T)]^{-1}; \tag{4}$$

for an overtone $2\upsilon_j$,

$$I \approx [1 - \exp(-1.44\upsilon_j/T)]^{-2}; \tag{5}$$

for a combination frequency $\upsilon_j + \upsilon_i$,

$$I \approx [1 - \exp(-1.44\upsilon_j/T)]^{-1} \times [1 - \exp(-1.44\upsilon_i/T)]^{-1}. \tag{6}$$

In our experimental observed intensities (Fig. 1), each integral intensity (I) has a negative temperature coefficient $\partial I/\partial T > 0$, which conflicts with the above theory. The reason is that there has been no direct consideration of the T dependence of I for the second harmonics. In similar cases of the compounds such as CCl_4, CS_2, C_6H_6, CH_3OH, and $C_2H_4Cl_2$, each of their second harmonics has a negative dI/dt.[27–29] Equations (5) and (6) indicate that I for overtone and combination frequency should increase with T more rapidly than for fundamental harmonics, which accord with the result that the experimentally observed fundamental harmonics differ in behavior from the overtones and combination in Fig. 2. The effect is related to molecular reorientation consequent on short-range order. When the molecular motion becomes more nearly free, this turns evident because the difference in I for the fundamental harmonic between the liquid and solid decreases as T increases. The T dependence is not linear and may be described fairly closely using activation energy U_{op} required for orientation change against the forces exerted by nearest neighbors.[24]

For $U_{op} < 1$ keal/mole, we express the I with the following equation as:

$$I = [1 - \exp(-1.44\nu_j/T)]^{-1} * e^{U_{op}/KT}. \quad (7)$$

Here, the values of U_{op} for CCl_4 and CS_2 are calculated from Eq. (7) using I data at the liquid–vapor transition, and show that they are in good agreement, which indicates that equation (7) is correct.[26] It enables us to predict the following features of the T dependence: negative dI/dT for all Stokes lines, since the $\exp(U_{op}/kT)$ factor decreases more rapidly than the second factor $[1 - \exp(-1.44\upsilon_j/T)]^{-1}$ in Eq. (7) increases. This fall in I should be virtually the same for all lines of a compound in a given range of T. The trends should also be roughly the same for fundamental harmonics and overtones/combination.

The $\exp(U_{op}/kT)$ factor means that the T dependence of I for second harmonic is taken into account. In our experiment, we observe that the liquid–solid phase transition appears at about -75 °C. The intensity ratios of the C–C overtone and combination to fundamental harmonic in the liquid and solid states have no obvious increase while they dramatically increase at the cirtical point of phase transition (Fig. 2). The T dependence of I has no direct relation to the dipole moment of the molecule nor to the refractive index, since here U_{op} is a decisive factor. As the orientation potential and molecular size usually govern the thermal motion. The rotational motion of larger molecules is to be treated as rotational diffusion. Compared with the more nearly free molecular motion in liquid, the rotational diffusion is damped by mixed solid molecules during the phase transition. Due to the fact that U_{op} means the orientation change of the activation energy against the force acting by the nearest neighbors, the U_{op} increases in the co-existing surrounding of liquid and solid molecules during phase transition. According to Eq. (7), the $\exp(U_{op}/kT)$ factor increases more rapidly and leads to a greater negative dI/dT during phase transition.

4.2. Geometry optimization and spectrum calculations

The fully optimized (unconstrained) structure of canthaxanthin, obtained by DFT calculations, is shown in Fig. 3. There is no strict rule of mutual exclusion; most of the modes display Raman activity. The calculated frequencies and Raman intensities are displayed in Table 1. A more detailed comparison reveals that the frequencies of most of the bands are reproduced by calculations with an average deviation. The calculated Raman intensities accord well with the experimental values except for the overestimations of some modes. Figure 4 shows the calculated Raman spectrum that accords very well with the experimental spectrum obtained with 514.5-nm excitation, except the peak at nearly 1525 cm^{-1}.

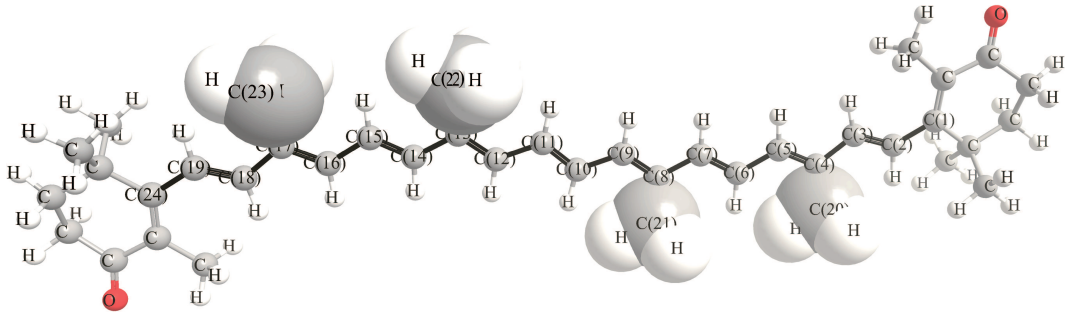


Fig. 3. (color online) Fully optimized polyene chain structure of canthaxanthin obtained by using the DFT method.

Table 1. Calculated frequencies and Raman intensities of the polyene chain structure of canthaxanthin.

Mode No.	Vibrational assignments (polyene chain)	Calculated frequencies	Intensities (I_{Ra})
1	C–H out of –plane (2); (3); (18); (19)	991	1.4
2	Methyl rock (20); (23)	1006	3.2
3	Methyl rock (21); (22)	1015	4.5
4	C–C str (11, 12); C–C str (9,10)	1153	3.8
5	C–C str (3, 4); (5, 6); (15,16); (17,18)	1166	64.8
6	C–H rock (2); (6); (10); (15); (19)	1283	5.7
7	C=C str (14, 15); (16, 17)	1307	1.6
8	C=C str (10, 11)	1316	0.8
9	C–H rock (3); (5); (7); (14); (16); (18)	1325	2.4
10	Asym methyl def. (21); (22)	1452	8.9
11	Asym methyl def. (20); (23)	1464	1.2
12	C=C str (8, 9); (12, 13)	1523	43.3
13	C=C str (6, 7); (10, 11); (14,15)	1531	100
14	C=C str (4, 5); (16, 17)	1580	1.7
15	C=C str (2, 3); (18, 19)	1586	5.5

[a] Relative Raman intensities with respect to the strongest Raman mode (13) that is normalized to 100. Frequencies less than 990 cm^{-1} and more than 1600 cm^{-1} are not shown.

In the region between 1800 cm^{-1} and 990 cm^{-1} which is considered in this work, the Raman-active modes can be grossly classified into five groups according to frequency and normal compositions. Between 1500 cm^{-1} and 1650 cm^{-1}, the C=C stretchings of the polyene chain make the main contributions to the modes, a closer inspection of the prominent band at 1523 cm^{-1}, however, reveals small but clearly detectable shifts of the peak maximum, among which the mode 1523 cm^{-1} is associated with the strongest Raman intensity 1531 cm^{-1}. The modes mainly involve the C–C stretching coordinates with the two most prominent modes 1153 cm^{-1} and 1166 cm^{-1} in the range of 1250 cm^{-1}–1150 cm^{-1}. Between 1500 cm^{-1} and 1400 cm^{-1}, the modes mainly involve methyl deformations and only a few of them exhibit appreciable Raman intensities, giving rise to a composite peak at 1452 cm^{-1}. The C–H rocking is the internal coordinate that dominates the modes between 1400 cm^{-1} and 1250 cm^{-1}, leading to an asymmetric peak at 1279 cm^{-1}. Finally, the methyl rocking prevails in the modes between 1050 cm^{-1} and 990 cm^{-1}.

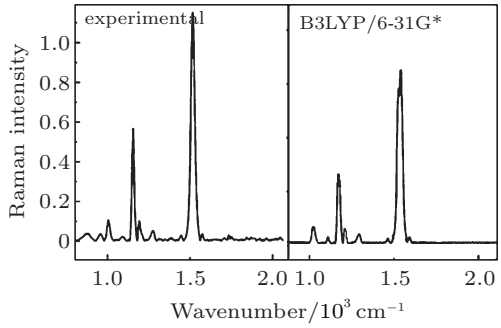


Fig. 4. Calculated Raman spectrum of canthaxanthin in the fully relaxed geometry (right) serving as a comparison with the experimental Raman spectrum obtained from a solution in 1,2-dichloroethane using 514.5-nm excitation (left).

Note that there is a prominent peak at nearly 1525 cm^{-1} consisting of two closely spaced modes based on above analyses. From viewing the characteristic structure of canthaxanthin in Fig. 3, one of C atoms in some specific CC double bond such as C_8=C_9, C_{12}=C_{13}, C_4=C_5, and C_{16}=C_{17} conjugates with an extra methyl compared with other CC double bonds. The C=C stretching of the polyene chain albeit with an alternating pattern, i.e. C_8=C_9 and C_{12}=C_{13} for 1523 cm^{-1}, C_4=C_5 and C_{16}=C_{17} for 1531 cm^{-1}, and C_2=C_3 and C_{18}=C_{19} for 1586 cm^{-1}, the different types of the C=C coordinates in the polyene chain are attributed to the distribution of wavenumbers. Additionally, the CC single bond stretchings of the adjacent methyl (C_3–C_4, C_5–C_6, C_{15}–C_{16}, C_{17}–C_{18}) for 1166 cm^{-1} are comparable to the stretchings of central isolated single bonds (C_9–C_{10} and C_{11}–C_{12}) for 1153 cm^{-1}. Meanwhile, the methyl coordinates in the polyene chain have an apparent effect on the C=C and C–C stretchings. Concomitantly, the lengths of the adjacent single bonds are reduced by about the same quantity, leading to nearly the same average bond length so that the single and double bonds of the polyene chain become very similar. Consequently, it may be possible that C–C stretching modes mix with the C=C stretching.

5. Conclusions

In this paper, the temperature-dependent resonance Raman spectra are measured in a temperature range from 20 °C to −180 °C. It is observed that all vibrational intensities of the polyene chain are inversely proportional to temperature, which is further analyzed by the resonance Raman effect and the coherent weakly damped electron/lattice vibrations. Meanwhile, it is observed that their combination and overtone intensities increase more rapidly with temperature than those of fundamental hamonics, and the results are discussed in detail with electron/phonon coupling and the activation energy U_{op}. Moreover, the polyene chain studies are complemented by the DFT B3LYP/6-31G* level. The calculated frequencies, compared with the experimentally observed spectral features, reflects a prominent peak at 1525 cm^{-1} that is composed of two closely spaced modes and both of them are dominated by C=C stretching coordinates of the polyene chain.

References

[1] Pfander H 1992 *Meth. Enzymol* **3** 213
[2] Mascio P D, Kaiser S and Sies H 1989 *Arch. Biochem. Biophys.* **274** 532
[3] Nishino H 1998 *Mutat. Res.* **402** 159
[4] Kette B 2001 *Photosynthesis–Photobiochemistry and Photobiophysics* (Dordrecht: Kluwer Academic Publishers) p. 10
[5] Guskov A, Kern J, Gabdulkhakov A, Broser M, Zouni A and Saenger W 2009 *Nat. Struct. Mol. Biol.* **16** 334
[6] Jordan P, Fromme P, Witt H T, Klukas O, Saenger W and Krauss N 2001 *Nature* **411** 909
[7] Mckenzie J L, Waid M C, Shi R Y and Webser T J 2004 *Biomaterials* **25** 1309
[8] Choudhury K R, Sahoo Y and Prasad P N 2005 *Adv. Mater.* **17** 2877
[9] Ryskulov A A, Liopo V A and Ovchinnikov E V 2011 *J. Frict. Wear* **32** 30
[10] Paraschuk D Y and Kobryanskii V M 2001 *Phys. Rev. Lett.* **87** 207402
[11] Mortensen A and Skibsted L H 1997 *J. Agric. Food. Chem.* **45** 2970
[12] Schliucker S, Szeghalmi A and Schmitt M 2003 *J. Raman. Spectrosc.* **34** 413
[13] Tian Y J, Zhang L Y, Zuo J, Li Z W and Gao S Q 2007 *Antal. Chim. Acta* **581** 154
[14] Tian Y J, Zuo J, Zhang L Y, Li Z W and Lu G H 2007 *Appl. Phys. B* **87** 727
[15] Koch W and Holthausen M C 2000 *A Chemists Guide to Density Functional Theory* (Weinheim: Wiley-VCH)
[16] Frisch M J, Truck G W, Schlegel H B, Scuseria G E, Robb M A, Cheeseman J R, Zakrzewski V G, Montgomery J A, Stratmann R E, Burant J C, Dapprich S, Millam J M, Daniels A D, Kudin K N, Strain M C, Farkas O, Tomasi J, Barone V, Cossi M, Cammi R, Mennucci B, Pomelli C, Adamo C, Clifford S, Ochterski J, Petersson G A, Ayala P Y, Cui Q, Morokuma K, Malick D K, Rabuck A D, Raghavachari K, Foresman J B, Cioslowski J, Ortiz J V, Boboul A G, Stefnov B B, Liu G, Liaschenko A, Piskorz P, Komaromi L, Gomperts R, Martin R L, Fox D J, Keith T, AlLaham M A, Peng C Y, Nanayakkara A, Gonzalez C, Challacombe M, Gill P M W, Johnson B, Chen W, Wong M W, Andres J L, Gonzalez C, Head-Gordon M, Replogle E S and Pople J A 2003 *GAUSSIAN* 03, revision A.1 end.; Guassian, Inc.: Pittsburgh, PA
[17] Magdo I, Nemeth K, Mark F, Hildebrandt P and Schaffner K 1999 *J. Phys. Chem.* **103** 289

[18] Mroginski M A, Murgida D H and Hildebrand t P 2006 *J. Phys. Chem. A* **110** 10564

[19] Fujii R, Chen C H, Mizoguchi T and Koyama Y 1998 *Spectrochim. Acta A* **54** 727

[20] Satito S and Tasumi M 1983 *J. Raman Spectrosc.* **14** 310

[21] Wu N N, Li Z W, Liu J Y and Ouyang S L 2012 *Chin. Phys. B* **21** 103101

[22] Castiglioni C, Zoppo M D and Zerbi G 1993 *J. Raman Spectrosc.* **24** 485

[23] Paraschuk D Y, Arnautov S A, Shchegolikhin A N and Kobryanskii V M 1996 *JETP Lett.* **64** 658

[24] Illinger H and Freeman D E 1962 *J. Mol. Spectrosc.* **9** 161

[25] Parker S F, Tavender S M and Dixon N M 1999 *Appl. Spectrosc.* **53** 1

[26] Stal'makhova L S, Sidorov N K and Kuryshin V I 1967 *Sovi. Phys. J.* **10** 75

[27] Sokolovskaya A I 1964 *Trudy. Fian.* **27** 63

[28] Bobovich Y S and Pirovarov V M 1957 *Opt. Spektr.* **3** 227

[29] Frenkel Y I 1959 *Selected Works* [in Russian], 3, Izd. AN SSSR, Moscow-Leningrad